Perfusional deficit and the dynamics of cerebral edemas in experimental traumatic brain injury using perfusion and diffusion-weighted magnetic resonance imaging

Anne Pasco [1] **, Laurent Lemaire** [1 *] **, Florence Franconi** [2] **, Yann Le Fur** [3] **, Fanny Noury** [1] **, Jean-Paul Saint-André** [4] **, Jean-Pierre Benoit** [1] **, Patrick J. Cozzone** [3] **, Jean-Jacques Le Jeune** [1]

[1] *Ingénierie de la vectorisation particulaire INSERM : U646 , Université d'Angers , Batiment IBT 10, Rue Andre Boquel 49100 ANGERS,FR*

[2] *SCAS-UNIV ANGERS, Service Commun d'Analyses Spectroscopiques Université d'Angers , UFR Sciences, 2 boulevard Lavoisier 49045 Angers cedex,FR*

[3] *CRMBM, Centre de résonance magnétique biologique et médicale CNRS : UMR6612 , Université de la Méditerranée - Aix-Marseille II , 27 Bvd Jean Moulin 13385 MARSEILLE CEDEX 05,FR*

[4] *Laboratoire d'Anatomie Pathologie CHU Angers , FR*

[*] Correspondence should be adressed to: Laurent Lemaire <laurent.lemaire@univ-angers.fr >

Abstract

The aim of this work was to characterize edema dynamics, cerebral blood volume and flow alterations in an experimental model of brain trauma using quantitative diffusion and perfusion MRI. Associated with an influx of water in the intracellular space 1–5hours post trauma as demonstrated by the 40% reduction in apparent diffusion coefficient, a 70–80% reduction in cerebral blood flow is measured within the lesioned region. Transient hypoperfusion (40–50%) was also observed in the non-traumatized contralateral hemisphere although there was no evidence of oedma formation. After the initial cytotoxic edema, a clear evolution toward extracellular water accumulation was observed, demonstrated by an increase in apparent diffusion coefficient.

MESH Keywords Animals ; Blood Flow Velocity ; physiology ; Blood Volume ; physiology ; Brain Edema ; etiology ; pathology ; physiopathology ; Brain Injuries ; complications ; pathology ; physiopathology ; Cerebrovascular Circulation ; physiology ; Contrast Media ; Diffusion Magnetic Resonance Imaging ; Female ; Meglumine ; diagnostic use ; Organometallic Compounds ; diagnostic use ; Rats ; Rats, Sprague-Dawley ; Time Factors

Author Keywords Traumatic brain injury ; Edema ; Quantitative magnetic resonance imaging ; Diffusion ; ADC ; Perfusion ; DSC ; Fluid lateral percussion.

Introduction

Traumatic brain injury (TBI) is a worldwide problem that results in death and disability for millions of people every year. Currently, in developed countries it is estimated that TBI is responsible for 1.5–2‰ of deaths and that 2–3% of the population lives with permanent disabilities (Thurman 1999 , Kay 2001 , Mathé 2005). Brain edema is the most common and serious consequence of traumatic brain injury and is associated with a poor neurological outcome (Sahuquillo 2001 , Leker 2002 , Unterberg 2004). Two different forms of edemas, namely, vasogenic and cytotoxic are co-existing in Cytotoxic edemas result from an osmotically-driven shift of water from the extra-cellular space into the cell (Klatzo 1987) as a consequence of ionic balance alteration, with concomitant cellular sodium influx and potassium efflux (Kawata 1995 , Reiner 2000). Conversely, vasogenic edemas occur with the extravasation of fluid into the extra-cellular space following transient blood brain barrier permeation. This may also promote or aggravate cell swelling.

MRI (DWI) was shown to be useful for the non-invasive assessment of brain water movement and to characterize brain edemas: cytotoxic edemas may be characterized by a reduced apparent diffusion coefficient (ADC), and vasogenic edemas by increased ADC values (Le Bihan 1986 , Huisman 2003 , Van putten 2005 , Pasco 2006). DWI has therefore been used in numerous longitudinal follow-ups of brain edema in TBI models, and a general trend shows post traumatic brain edema to be a combination of both vasogenic and cytotoxic edemas with a predominant cellular component (Ito 1996 , Barzo 1997 , Beaumont 2000 , Albensi 2000 , Schneider 2002 , Van Putten 2005).

Metabolic perturbations associated with brain edema formation are reported in TBI (Levasseur JE 2000 , Reinert 2004 , Viant 2005 , Bauman 2005) and may at least in part be the result of decreased brain perfusion. MRI may also be used for the non-invasive assessment of brain perfusion using dynamic susceptibility contrast magnetic resonance imaging (DSC-MRI) after a bolus injection of contrast agent (Ostergaard 1996a). In the brain, the first-pass extraction of the contrast agent is zero when the blood-brain barrier is reasonably intact, and the intravascular compartmentalization of the contrast agent creates strong, microscopic susceptibility gradients. These microscopic gradients cause the dephasing of the spins which diffuse among these gradients, resulting in signal loss in T2- and T*2-weighted images (Villringer 1988) proportional to the contrast agent concentration (Simonen 1999). Therefore, the kinetic analysis of the concentration time curves while dynamically tracking the passage of a bolus of high-susceptibility contrast agent, may be used to determine Cerebral Blood Volume (CBV) and Flux (CBF) as well as mean transit time (MTT) [Ostergaard 1996b, Ostergaard 1998].

The purpose of the present study is to provide a better understanding of the time course of edemas formation associated with TBI using DWI, and to assess early perfusion alteration using DSC-MRI in an experimental animal model.

Materials and Methods

Fluid percussion-induced brain injury

Animal care was carried out in compliance with the relevant European Community regulations (Official Journal of European Community L358 12/18/1986).

230–270 g female Sprague–Dawley rats where supplied by Angers University Hospital animal facility); they were anaesthetized with isoflurane via a stereotactic compatible nose cone (Minerve, Esternay, France), being induced at 5% and maintained at 1.5% throughout the entire procedure. Once induced, the animal was placed in a stereotactic frame. A scalp incision was made, the scalp and temporal muscles were reflected, and a 2.5mm craniotomy was carried out above the left auditory cortex, 2mm posterior to the lateral suture. A fitting tube, connected to the fluid lateral percussion device was cemented into the open craniotomy site. A 20 ms pulse at a pressure of 2.0 ± 0.1 atm induced fluid lateral percussion brain injury. Immediately after fluid lateral percussion, the scalp incision was sutured and the rats were allowed to recover from anaesthesia. Normothermia was maintained through the use of a heating pad placed under the animal during all surgical procedures and in the acute post-injury period. The temperature was maintained between 36.5°C and 37.5°C.

Thereafter, rats were housed in temperature- and light-controlled conditions with food and water ad libitum. Sham-operated rats underwent the same surgery except for percussion.

MR imaging protocol

Experiments were performed with a Bruker Avance DRX 300 (Bruker, Wiessembourg, France) equipped with a vertical superwide-bore magnet and shielded gradient insert. The resonant circuit of the nuclear magnetic resonance (NMR) probe was a 38 mm diameter birdcage. Rectal temperature was maintained between 36.5°C and 37.5°C by using a feedback-regulated heating pad.

Each animal was scanned at least three times (2h, 5h and 3 days or 7 days post TBI) for brain lesions. Evolution was assessed using T2 weighted, FLAIR and diffusion imaging. Post-trauma diffusion values were then measured after 2h (n = 6), 5 h (n = 5), 3 days (n = 4) and 7 days (n = 3).

Qualitative T2-weighted images were obtained using a rapid acquisition with relaxation enhancement (RARE) (Henning 1986) (TR = 2,000 ms; effective echo time = 31.7 ms; RARE factor = 8; FOV = 3 × 3 cm; matrix 128 × 128; nine contiguous slices of 1 mm, eight averages). FLAIR imaging was performed using a 600ms inversion pulse prior to the RARE pattern, allowing enough time to cancel normal parenchyma and therefore edema detection (Vonarbourg 2004).

A 3-mm thick diffusion-weighted image was taken, located at the center of the lesion. In order to reach an acceptable signal-to-noise ratio without dramatically increasing the acquisition time, a 96 × 96 matrix for FOV = 3 × 3 cm was used, leading to an in-plane resolution of 312μm. Diffusion images were obtained using a Stejskal-Tanner-type pulsed gradient stimulated echo sequence (Stejskal 1965) with four diffusion weighting factor values (b)=[b = $(\gamma G\delta)^2$ $(\Delta-\delta/3)$], with γ = gyromagnetic ratio, G: gradient strength = 100ms, δ: gradient duration = 5ms, Δ = duration between the leading edges and b = 95, 307, 770, 1484 s/mm^2 . The diffusion-sensitizing gradient was placed only along the direction of the slice selection gradient (i.e. rostrocaudally) regardless of the usual practice of calculating the ADC from a set of at least three orthogonal directions in order to reduce potential pitfalls due to brain anisotropy. We based our decision to make ADC calculation on a single direction on Van Putten's results in a TBI model showing no anisotropy (Van putten 2005) and on Lythogoe's results showing that in rat parietal cortex (Lythgoe 1997), the trace value calculated from the three orthogonal sets was close to the value measured with the diffusion gradient positioned rostrocaudally. The imaging time was then limited to about 15 minutes.

In order to improve image quality, ECG synchronisation was performed (Rapid Biomed, Wurzburg, Gernamy) and two averages were recorded. The minimal TR was set to 1,000ms whereas, TE and mixing time (TM) were set at TE/TM = 22.7/88.1 ms.

DSC-MRI perfusion measurements post-trauma were performed on separate animals at 1–2h (n=5), 4–5h (n=5) and 2–3days (n=3) using fast, low-angle snapshot (FLASH) (Haase 1990) gradient echo acquisitions (TR/TE/α = 18ms/10ms/10°), and a bolus injection of 150μl Dotarem®, injected after 10 images with a temporal resolution of 1.1 s per image.

Blood brain barrier (BBB) permeability was assessed by intravenous injection via the tail vein of 150 μl of commercial Dotarem® (Guerbet, Aulnay sous bois, France) using a set of two spin-echo sequences (TR/TE = 400/7ms) performed prior to and 10–12 minutes post injection. Scans geometry was identical to the geometry used for T2-weighted images. Five rats were images within 5 hours post-trauma,

three on day 3–4 post-trauma and two at a week post trauma. When no obvious contrast enhancements were visually detectable, a semi-quantitative approach was taken by measuring relative enhancement on a pixel to pixel basis. Enhancement profiles were then displayed for a region of interest (ROI) encompassing the lesion and its symmetrical counterpart taken in the contra-lateral hemisphere.

Generation of hemodynamic parameter and diffusion maps

ADC maps were calculated by mono-exponential fitting of the experimental points using Bruker Paravision 2.0® software. Quantitative haemodynamic parameters from DSC-MRI images were obtained using a gamma-variate fit, including an arterial input function (Østergaard 1996a) derived from the internal carotid ipsilateral to the lesion. Calculations were performed in IDL (Interactive Data Language, Research Systems, Boulder, CO, USA) using in-house-software (Centre de Résonance Magnétique Biologique et Médicale, Marseille, France). Further analysis was performed on ROI basis, ROIs being placed within the lesioned cortex, and at the same level but within the contra-lateral hemisphere.

Statistical analysis

Data is expressed as mean ± sem. Statistical analysis was performed using a bi-factorial analysis of variance (ANOVA) with a multiple-least-square analysis.

Brain lesion

A classical histological evaluation of rat brain lesion was performed on day 0, day 1, day 3, and day 7, using haematein-eosin and Perls staining. Brain water content (BWC) was determined in sham-operated rats (n=3), and 3h (n = 3), 24 (n = 3) and 48 h (n = 3) post-trauma using the wet weight–dry weight technique. Rapid brain removal was performed and 2–3 mm slices were dissected directly above craniotomy, the ispi and contralateral brain were separated. After weighing, samples were frozen lyophilized. The percentage of water content was then calculated and compared to the water content of the sham-operated rats.

The BWC was calculated as follows:

$$BWC = 100 \times \frac{(wet\,weight - dry\,weight)}{(wet\,weight)}$$

Results

Brain water content

Water content (Figure 1) in sham-operated animals was equivalent in the 3mm slices taken above craniotomy in the left and right hemispheres (p = 0.26) and equalled 74.6 ± 1.2 % (n = 6). On the ipsi-lateral side of the impact, the water content tended to increase compared to sham-operated animals (+4.2% on t = 24h, p = 0.058) to reach significance by t = 48h (+9.2%, p = 0.001). On the contralateral side, water content remained stable up to 24h (+ 1.5%, p = 0.46) and increased (+ 6.0%, p = 0.02) by t = 48h. Water content in the ipsilateral hemisphere significantly increased compared to the contralateral hemisphere by t = 24h (+5.3%, p = 0.012) and t = 48h (+6.5%, p = 0.019).

MR imaging – T1, T2 and FLAIR imaging

The lesioned cortex was detected at the first MRI examination occurring about 1-hour post-TBI; it showed as a hyperintense area on RARE and FLAIR images (Figure 2). On T1-weighted images, no signal changes were observed prior to contrast agent injection and the enhancement representative of BBB leakage was only observed from D3-4 post-TBI (Figure 3).

MR imaging – Diffusion

DW images showed a lesion encompassing both the auditory and parietal cortex (figure 4a). Quantitative analyses of DW images reported in Table 1 , summarize ADC values for the lesioned cortex and the contralateral cortex at 1–2h, 4–5h, 24h, 72h and 1 week after TBI. In the contralateral hemisphere, ADC values measured symmetrically to the lesioned cortex remained stable throughout the entire experimental time at an average ADC value of 0.597 ± 0.015 × 10^3 mm^2 /s (n=20). Within the lesioned cortex, a massive and rapid decrease in ADC was observed with an averaged ADC value of 0.399 ± 0.042 × 10^3 mm^2 /s at t =1–2h which gradually increased to reach 0.854 ± 0.132 × 10^3 mm^2 /s at 1 week.

MR imaging - Perfusion

Reliable quantitative DSC-imaging requires reasonably intact BBB and therefore minimal contrast agent leakage. BBB status was therefore assessed using late enhancement on T1-weighted images using Dotarem®. The qualitative analysis of post-contrast injection images (Figure 3 a, c,d and f) showed an evident enhancement and therefore BBB leakage from day 3–4 post TBI. A semi-quantitative analysis of the images was performed by displaying the distribution of the number of pixels with respect to their enhancement in order to

objectively evaluate the enhancement or more especially the non-enhancement observed earlier. At the later post-trauma times (figure 3e), profiles were different between the contra- and ipsi-lateral brain, confirming that enhancement only occurred ipsi-laterally to the impact. At earlier times, profiles were identical in both hemispheres and revealed that about 90% of the pixels experienced an enhancement of < 25 % (Figure 3b). Therefore, quantitative parameters such as CBF, CBV and MTT were only calculated on 1–2h, 4–5h, and 2–3 days post TBI (Table 1). Qualitative analysis of CBV, CBF or MTT maps unambiguously localized the brain lesions (figure 4b–d). On non-traumatized animals, CBF, CBV and MTT were identical for both hemispheres and respectively equal to 125.4 ± 5.5 ml/100g/min, 13.7 ± 1.4 ml/100g and 8.0 ± 0.2 s. In the contralateral hemisphere of TBI rats, MTT and CBV remained unchanged throughout the experimental time whereas a significant decrease in CBF was observed 1–2hours and 4–5hours post-trauma, respectively (50%, p =0.01 and 37% p=0.047). On the ipsilateral side, MTT increased respectively by 31% (p = 0.04), 59% (p = 0.02) and 80% (p = 0.01) 1–2, 4–5hours and 3 days post trauma. After an initial significant reduction in CBF (1–2h, 70% (p = 0.0001); 4–5h, 76% (p = 0.0001)) and in CBV (1–2h, 50% (p = 0.003); 4–5h, 58% (p = 0.002)), normalization was observed by day 3.

Histology

As early as 3 hours post-trauma, a cortical edema was depicted on histological slices with limited haemorrhage. An evident interstitial edema was observed by day 1 and macrophage infiltration by day 3. By day 7, this infiltration increased, and was associated to gliosis and haemosiderin. No contralateral lesions were observed.

Discussion

The purpose of the present study was to provide a better understanding of the time course of edemas formation associated with TBI using DWI, and to assess early perfusion alteration using DSC-MRI.

Brain trauma is a dynamic process characterized by two waves of lesions (Sahuquillo 2001 , Laurer 2000). The first wave encompasses the immediate mechanical damage to the central nervous system that occurs at the moment of impact, and the second wave, initiated at the moment of the traumatic insult, will progresses over time. In severe brain traumas, the mechanical impact itself triggers a massive release of glutamate and neuronal depolarization (traumatic depolarization) with secondary impairment of energy metabolism, with consequences on ionic homeostasis and cellular edema. However, TBI encloses by two forms of edemas. Vasogenic edemas, related to the structural lesions of vascular endothelium and to the accumulation of water and plasmatic fluid in the extracellular space, and intracellular edemas related to post-traumatic depolarization, glutamate excitotoxicity and the failure of brain energy production.

Brain water content (BWC) assessed invasively by comparing the wet/dry weight of the brain is increased significantly 24hours post TBI. Both hemispheres were affected, but largely at the ipsilateral level in relation to the trauma (Figure 1) as previously reported in the weight drop impact-acceleration model of trauma in mice (Beni-Adani 2001) and rats (Barzo 1997 , Beaumont 2006) or in a fluid lateral percussion model in rats (Besson 2005). Water distribution was also assessed non-invasively using quantitative diffusion MRI. This technique was proven useful in characterizing both intra- and extracellular edema in rats (Ito 1996 , Van Putten 2005) and in humans (Pasco 2006 , Marmarou 2000 , Hergan 2002). Thus, subtle changes that are not detectable using the wet/dry weight of the brain method are seen (Table 1). The decrease in ADC observed 1–2hours post-TBI, characteristic of intracellular edemas, illustrates the cellular swelling consecutive to TBI and is in perfect agreement with previously published works (Assaf 1999 , Albensi 2000 , Van Putten 2005). However, a transient initial increase of ADC was also reported in the fluid lateral percussion or in the impact-acceleration models of TBI, but in those cases the TBI appeared to be of higher magnitude (Barzo 1997 , Hanstock 1994). After the initial reduction of ADC, a slight increase was observed on day 1, ‘normalization' by day 3 and significant increase by 1week. The ‘normalization' observed by day 3 in fact reflects the natural evolution of the lesion from a predominant intracellular edema to an extracellular edema (Assaf 1999 , Barzo 1997). Compared to the reported ADC evolution in human TBI (Pasco 2006), a similar trend was observed, the only difference being that the kinetics was faster.

Associated with the 40% reduction in ADC 1–2 hours post TBI, a massive modification in perfusional parameters was observed in both hemispheres (Table 1), the lesioned hemisphere being the most affected (Figure 4). Indeed, the most affected parameter, i.e. CBF, was reduced by 70–80% 1–5 hours post TBI in the hemisphere experiencing the fluid lateral percussion and by 40–50% in the contralateral hemisphere as previously described in fluid lateral percussion (Yamakami 1991), controlled cortical impact (Hendrich KS 1999) or in impact-acceleration (Assaf 1999) induced injury. However, as observed for ADC, the magnitude of TBI has a major effect on perfusion parameters changes. Thus, a light trauma, i.e. < 1atm, does not induce changes in CBF in the contralateral hemisphere and a maximal reduction of 22% 8 hours post-TBI (Schneider 2002). Interestingly, and despite the massive reduction in CBF within the contra-lateral brain that lasted for at least 2 hours, no ischemic-like lesions were depicted in this hemisphere. Such a phenomenon seems to be a constant in fluid lateral percussion (Yamakami 1991), controlled cortical impact (Hendrich KS 1999), impact-acceleration (Assaf 1999) or even focal cerebral ischemia injury models (Shen 2005a , Windle 2006). However, the brain perfusion deficit associated to brain swelling is deleterious for the brain. A recent study dealing with tissue fate with respect to CBF and ADC changes conducted in a permanent middle cerebral artery model shows that the statistical analysis of the combination of ADC and CBF maps may predict tissue fate. (Shen 2005b)

Three days post-fluid lateral percussion, the dispersion of CBF values did not show a significant reduction ($p = 0.12$). Despite an average reduction of 30%, the tendency to normalization tallied with Yamakami's observations (Yamakami 1991). Concerning CBV and MTT, changes only occurred in the ipsilateral hemisphere: a reduction of about 50–60% 2–5 hours post-TBI for CBV and an increase of the same magnitude for MTT. On day 3, tendency to normalization was also observed.

Conclusions

Taken altogether and as displayed in figure 5 , trends in BWC, ADC and perfusion evolution indicate that massive and rapid edema occurs after moderate TBI induced by fluid lateral percussion. Associated to an influx of water in the intracellular space 1–5hours post fluid lateral percussion as demonstrated by the ADC reduction in the TBI region, a global reduction in perfusion parameters is observed in both hemispheres. Perfusion alterations are however slighter in the contralateral brain. After a predominant intracellular edema, an increase of the water content within the lesioned brain is measured using the invasive wet/dry weight method whereas non-invasive quantitative diffusion MRI localizes the water excess in the extracellular space.

Ackowledgements:

We wish to thank Valérie Besson and Catherine Marchand-Verrecchia from the Laboratoire de Pharmacologie de la Circulation Cérébrale, UPRES EA 2510, Université Paris Descartes, for providing us with the lateral fluid percussion injury model and F BoulaBiar for editing the text. This work was supported in part by a grant from 'la Fondation des Gueules Cassées', Paris, France.

References:

- Albensi BC , Knoblach SM , Chew BG , O'Reilly MP , Faden AI , Pekar JJ . 2000 ; Diffusion and high resolution MRI of traumatic brain injury in rats: time course and correlation with histology . Exp Neurol . 162 : 61 - 72
- Assaf Y , Holokovsky A , Berman E , Shapira Y , Shohami E , Cohen Y . 1999 ; Diffusion and perfusion magnetic resonance imaging following closed head injury in rats . J neurotrauma . 16 : (12) 1165 - 76
- Barzo P , Marmarou A , Fatouros P , Hayasaki K , Corwin F . 1997 ; Contribution of vasogenic and cellular edema to traumatic brain swelling measured by diffusion-weighted imaging . J Neurosurg . 87 : 900 - 907
- Bauman RA , Widholm J , Long JB . 2005 ; Secondary hypoxia exacerbates acute disruptions of energy metabolism in rats resulting from fluid percussion injury . Behav Brain Res . 160 : (1) 25 - 33
- Beaumont A , Marmarou A , Hayasaki K , Barzo P , Fatouros P , Corwin F , Marmarou C , Dunbar J . 2000 ; The permissive nature of blood brain barrier (BBB) opening in edema formation following traumatic brain injury . Acta Neurochir Suppl . 76 : 125 - 129
- Beaumont A , Fatouros P , Gennarelli P , Corwin F , Marmarou A . 2006 ; Bolus tracer delivery measured by MRI confirms edema without blood-brain barrier permeability in diffuse traumatic brain injury . Acta Neurochir Suppl . 96 : 171 - 4
- Beni-Adani L , Gozes I , Cohen Y , Assaf Y , Steingart RA , Brenneman DE , Eizenberg O , Trembolver V , Shohami E . 2001 ; A peptide derived from activity-dependent neuroprotective protein (ADNP) ameliorates injury response in closed head injury in mice . J Pharmacol Exp Ther . 296 : (1) 57 - 63
- Besson VC , Chen XR , Plotkine M , Marchand-Verrecchia C . 2005 ; Fenofibrate, a peroxisome proliferator-activated receptor alpha agonist, exerts neuroprotective effects in traumatic brain injury . Neurosci Lett . 388 : (1) 7 - 12
- Haase A . 1990 ; Snapshot FLASH MRI. Applications to T1, T2, and chemical-shift imaging . Magn Reson Med . Jan 13 : (1) 77 - 89
- Hanstock CC , Faden AI , Bendall MR , Vink R . 1994 ; Diffusion-weighted imaging differentiates ischemic tissue from traumatized tissue . Stroke . 25 : (4) 843 - 8
- Hendrich KS , Kochanek PM , Williams DS , Schiding JK , Marion DW , Ho C . 1999 ; Early perfusion after controlled cortical impact in rats: quantification by arterial spin-labeled MRI and the influence of spin-lattice relaxation time heterogeneity . Magn Reson Med . 42 : (4) 673 - 81
- Hennig J , Nauerth A , Friedburg H . 1986 ; RARE imaging: a fast imaging method for clinical MR . Magn Reson Med . 3 : (6) 823 - 33
- Hergan K , Schaefer PW , Sorensen AG , Gonzalez RG , Huisman TA . 2002 ; Diffusion-weighted MRI in diffuse axonal injury of the brain . Eur Radiol . 12 : 2536 - 2541
- Huisman TA . 2003 ; Diffusion-weighted imaging: basic concepts and application in cerebral stroke and head trauma . Eur Radiol . 13 : 2283 - 2297
- Ito J , Marmarou A , Barzo P , Fatouros P , Corwin F . 1996 ; Characterization of edema by diffusion-weighted imaging in experimental traumatic brain injury . J Neurosurg . 84 : 97 - 103
- Kawamata T , Katayama Y , Hovda DA , Yoshino A , Becker DP . 1995 ; Lactate accumulation following concussive brain injury: the role of ionic fluxes induced by excitatory amino acids . Brain Research . 674 : 196 - 204
- Kay A , Teasdale G . 2001 ; Head injury in the United Kingdom . J Surg . 25 : 1210 - 1220
- Klatzo I . 1987 ; Pathophysiological aspects of brain edema . Acta Neuropathol (Berl) . 72 : 236 - 239
- Laurer HL , Lenzlinger PM , McIntosh TK . 2000 ; Models of traumatic brain injury . Eur J Trauma . 26 : 995 - 1000
- Le Bihan D , Breton E , Lallemand D , Grenier P , Cabanis E , laval-Jantet M . 1986 ; MR imaging of intravoxel incoherent motions: application to diffusion and perfusion in neurologic disorders . Radiology . 161 : 401 - 407
- Leker RR , Shohami E . 2002 ; Cerebral ischemia and trauma-different etiologies yet similar mechanisms: neuroprotective opportunities . Brain Res Brain Res Rev . 39 : 55 - 73
- Levasseur JE , Alessandri B , Reinert M , Bullock R , Kontos HA . 2000 ; Fluid percussion injury transiently increases then decreases brain oxygen consumption in the rat . J Neurotrauma . 17 : 101 - 112
- Lythgoe MF , Busza AL , Calamante F , Sotak CH , King MD , Bingham AC , Williams SR , Gadian DG . 1997 ; Effects of diffusion anisotropy on lesion delineation in a rat model of cerebral ischemia . Magn Reson Med . Oct 38 : (4) 662 - 8
- Marmarou A , Fatouros PP , Barzo P , Portella G , Yoshihara M , Tsuji O , Yamamoto T , Laine F , Signoretti S , Ward JD , Bullock MR , Young HF . 2000 ; Contribution of edema and cerebral blood volume to traumatic brain swelling in head-injured patients . J Neurosurg . 93 : 183 - 193
- Mathé JF , Richard I , Rome J . 2005 ; Santé publique et traumatisme crâniens graves. Aspects épidémiologiques et financiers, structures et filières de soins . Ann Fr Anesth Reanim . 24 : (6) 688 - 94
- Østergaard L , Weisskoff RM , Chesler DA , Gyldensted C , Rosen BR . 1996 ; High resolution measurement of cerebral blood flow using intravascular tracer bolus passages. Part I: Mathematical approach and statistical analysis . Magn reson Med . 36 : (5) 715 - 25
- Østergaard L , Sorensen AG , Kwong KK , Weisskoff RM , Gyldensted C , Rosen BR . 1996 ; High resolution measurement of cerebral blood flow using intravascular tracer bolus passages. Part II: Experimental comparison and preliminary results . Magn Reson Med . 36 : (5) 726 - 36
- Østergaard L , Smith DF , Vestergaard-Poulsen P , Hansen SB , Gee AD , Gjedde A , Gyldensted C . 1998 ; Absolute cerebral blood flow and blood volume measured by magnetic resonance imaging bolus tracking: comparison with positron emission tomography values . J Cereb Blood Flow Metab . 18 : 425 - 432

- Pasco A , Ter Minassian A , Chapon C , Lemaire L , Franconi F , Darabi D , Caron C , Benoit JP , Le Jeune JJ . 2006 ; Dynamics of cerebral edema and the apparent diffusion coefficient of water changes in patients with severe traumatic brain injury. A prospective MRI study . Eur Radiol . 16 : (7) 1501 - 8
- Reinert M , Khaldi A , Zauner A , Doppenberg E , Choi S , Bullock R . 2000 ; High level of extracellular potassium and its correlates after severe head injury: relationship to high intracranial pressure . J Neurosurg . 93 : (5) 800 - 7
- Reinert M , Schaller B , Widmer HR , Seiler R , Bullock R . 2004 ; Influence of oxygen therapy on glucose-lactate metabolism after diffuse brain injury . J Neurosurg . 101 : (2) 323 - 9
- Sahuquillo J , Poca MA , Amoros S . 2001 ; Current aspects of pathophysiology and cell dysfunction after severe head injury . Curr Pharm Des . 7 : 1475 - 1503
- Schneider G , Fries P , Wagner-Jochem D , Thome D , Laurer H , Kramann B , Mautes A , Hagen T . 2002 ; Pathophysiological changes after traumatic brain injury: comparison of two experimental animal models by means of MRI . Magn Reson Phys Mater . 14 : 233 - 241
- Shen Q , Ren H , Cheng H , Fisher M , Duong TQ . 2005a ; Functional, perfusion and diffusion MRI of acute focal ischemic brain injury . J Cereb Blood Flow Metab . 25 : (10) 1265 - 79
- Shen Q , Ren H , Fisher M , Duong TQ . 2005b ; Statistical prediction of tissue fate in acute ischemic brain injury . J Cereb blood Flow . 25 : 1336 - 1345
- Stejskal EO , Tanner JE . 1965 ; Spin diffusion measurements: spin-echoes in the presence of a time-dependent field gradient . J Chem Phys . 42 : 288 - 292
- Simonsen CZ , Østergaard L , Vestergaard-Poulsen P , Rohl L , Bjornerud A , Gyldensted C . 1999 ; CBF and CBV measurements by USPIO bolus tracking: reproducibility and comparison with Gd-based values . J Magn Reson Imaging . 9 : 342 - 347
- Thurman DJ , Alverson C , Dunn KA , Guerrero J , Sniezek JE . 1999 ; Traumatic brain injury in the United States: a public health perspective . J Head Trauma Rehabil . 14 : 602 - 615
- Unterberg AW , Stover J , Kress B , Kiening KL . 2004 ; Edema and brain trauma . Neuroscience . 129 : 1021 - 1029
- Van Putten HP , Bouwhuis MG , Muizelaar JP , Lyeth BG , Berman RF . 2005 ; Diffusion-weighted imaging of edema following traumatic brain injury in rats: effects of secondary hypoxia . J neurotrauma . 22 : (8) 857 - 72
- Viant MR , Lyeth BG , Miller MG , Berman RF . 2005 ; An NMR metabolomic investigation of early metabolic disturbances following traumatic brain injury in a mammalian model . NMR Biomed . 18 : (8) 507 - 16
- Villringer A , Rosen BR , Belliveau JW , Ackerman JL , Lauffer RB , Buxton RB , Chao YS , Wedeen VJ , Brady TJ . 1988 ; Dynamic imaging with lanthanide chelates in normal brain: contrast due to magnetic susceptibility effects . Magn Reson Med . 6 : 164 - 174
- Vonarbourg A , Sapin A , Lemaire L , Franconi F , Menei P , Jallet P , Le Jeune JJ . Characterization and detection of experimental rat gliomas using magnetic resonance imaging, (2004) . Magn Reson Phys Mater . 2004 ; 17 : (3–6) 133 - 9
- Windle V , Szymanska A , Granter-Button S , White C , Buist R , Peeling J , Corbett D . An analysis of four different methods of producing focal cerebral ischemia with endothelin-1 in the rat . Exp Neurol . 2006 ; 2001 : 324 - 334
- Yamakami I , McIntosh T . 1991 ; Alterations in regional cerebral blood flow following brain injury in the rat . J Cereb Blood Flow Metab . 11 : 655 - 660

Figure 1

Evolution of the Brain Water Content (BWC) for the ipsilateral (•) and contral-lateral (○) tissue to FPI as a function of post-trauma time.

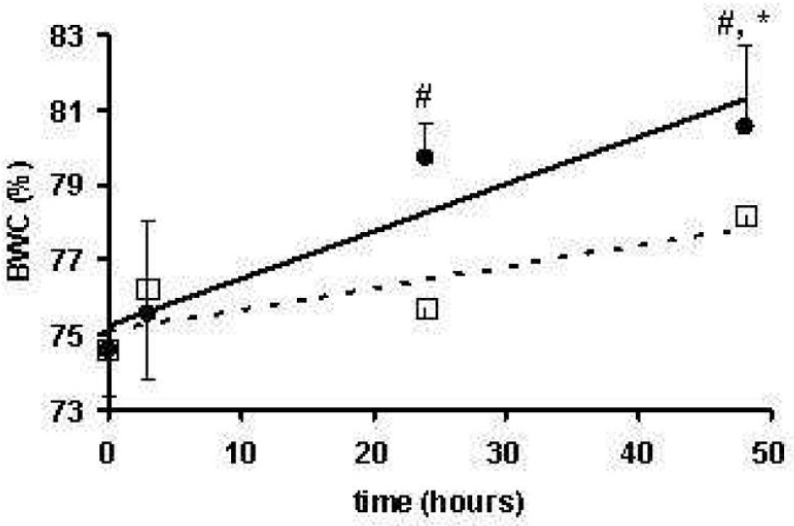

Figure 2

Four contiguous, T2-weighted images obtained using a rapid acquisition with relaxation enhancement (RARE) sequence (right column) and the corresponding slices obtained with the inclusion of an inversion pulse of 600ms prior to the RARE pattern in order to cancel the signal of normal parenchyma (left column).

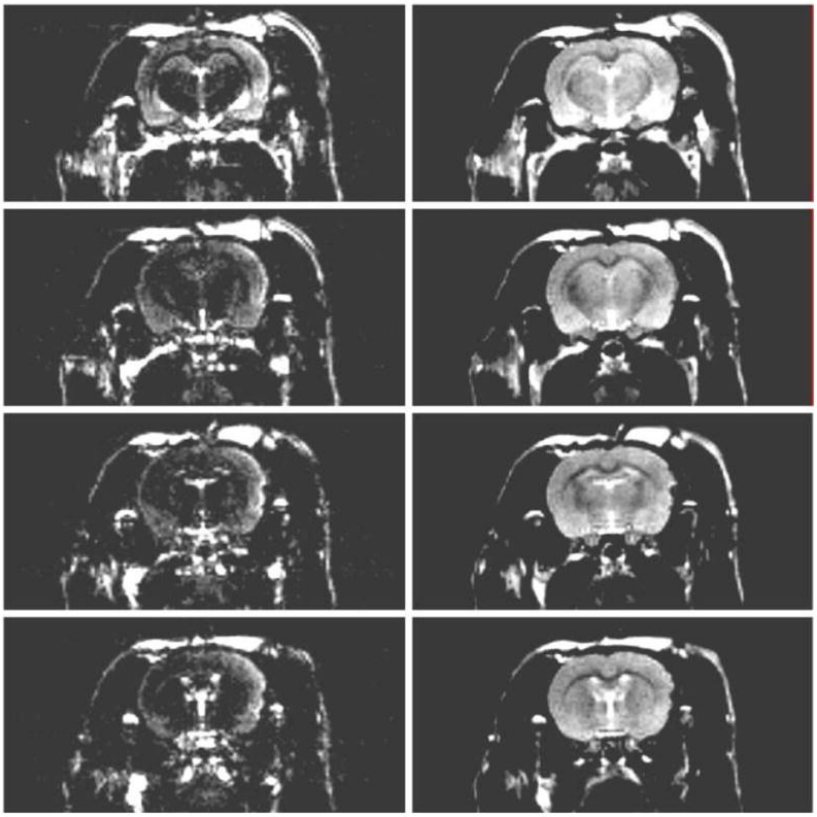

Figure 3

Evaluation of the Blood Brain Barrier leakage as a function of time (a) 2hours, (c) 5 hours, (d) 3 days and (f) 7 days post-trauma using a Gadolinium chelate injection. Frames (b) and (e) correspond respectively to the semi-quantitative analysis of images presented in frames (a) and (d). The dashed bars represent the ipsilateral brain and the white bars the contralateral brain.

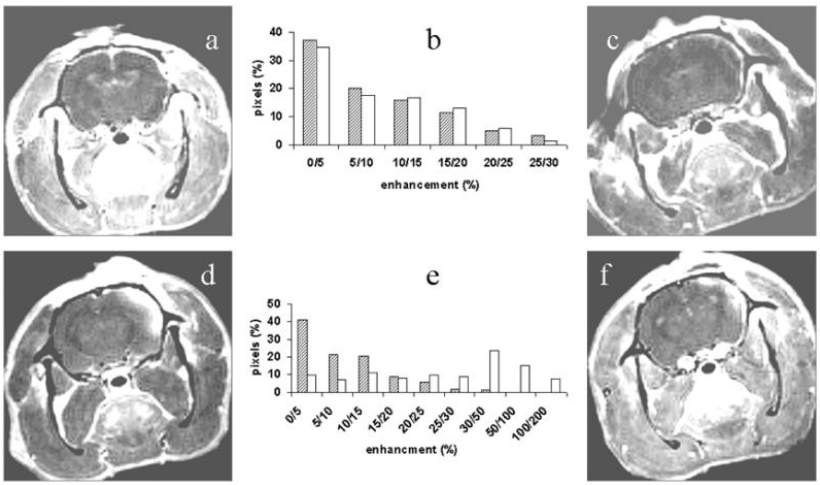

Figure 4

Typical quantitative images of a rat brain 3hours post-TBI. ADC map (upper left) CBF map (upper right), CBV (lower left) and MTT (lower right) are presented.

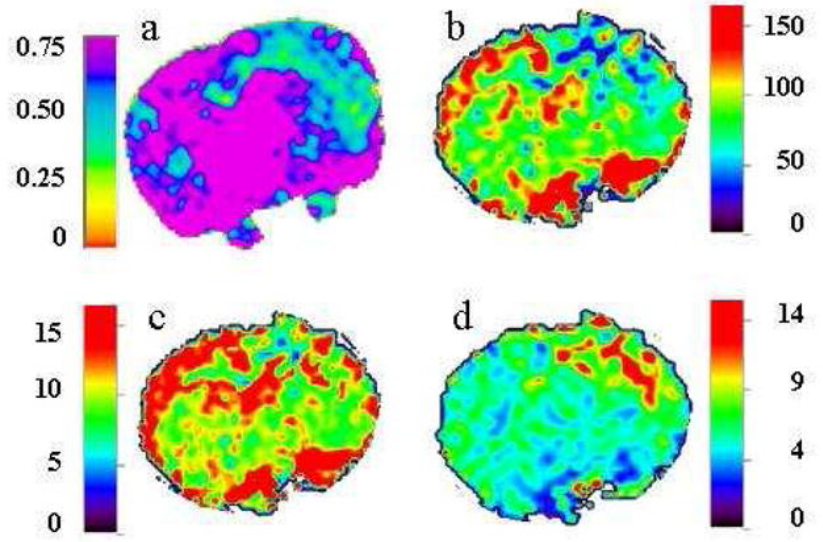

Figure 5

Trends in ADC (—•— ipsilateral; ---○--- contralateral) and CBF (—■— ipsilateral; ---□--- contralateral) evolution in rat brain after a mild traumatic brain injury.

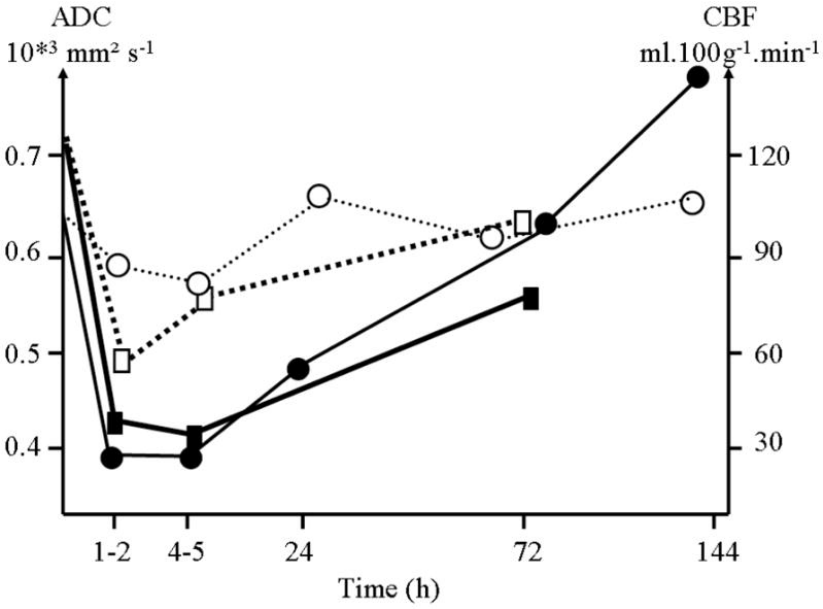

Table 1

ADC, CBF, CBV, and MTT evolution as a function of time after TBI in ipsi and contralateral rat brain. Data are presented as mean ± sem.

		Sham operated	1–2h	4–5h	24h	72h	1Wk
IPSILATERAL CORTEX	ADC (x 10^3 mm^2 $.s^{-1}$)	0.670 ± 0.026	0.399 ± 0.042 *,#	0.396 ± 0.033 *,#	0.486 ± 0.158 *,#	0.637 ± 0.073	0.852 ± 0.132 *,#
	CBF (ml.100g^{-1} .min^{-1})	119.9 ± 12.6	36.1 ± 4.7 *,#	29.0 ± 4.4 *,#	nd	83.0 ± 29.1	nd
	CBV (ml.100g^{-1})	15.0 ± 2.6	7.38 ± 0.8#	6.4 ± 0.5#	nd	15.0 ± 4	nd
	TTM (s)	7.8 ± 0.6	10.2 ± 1.4	12.4 ± 1.5#	nd	12.0 ± 2.0	nd
CONTRALATERAL CORTEX	ADC (x 10^3 mm^2 $.s^{-1}$)	0.620 ± 0.047	0.595 ± 0.020	0.544 ± 0.022	0.665 ± 0.033	0.603 ± 0.038	0.640 ± 0.076
	CBF (ml.100g^{-1} .min^{-1})	130.8 ± 29.1	57.7 ± 5.7*	81.8 ± 11.6*	nd	97.6 ± 11.4	nd
	CBV (ml.100g^{-1})	12.3 ± 1.4	9.0 ± 1.0	8.7 ±0.6	nd	14.0 ± 2.1	nd
	TTM (s)	8.2 ± 0.6	8.4 ± 0.5	7.1 ± 0.9	nd	10.2 ± 1.5	nd

* significantly different from sham operated values

significantly different from contralateral values at the same time point.